Power Engineering and Engineering Thermophysics
https://www.acadlore.com/journals/PEET

Energy and Exergy Evaluation of a Dual Fuel Combined Cycle Power Plant: An Optimization Case Study of the Khoy Plant

Razieh Abbasgholi Rezaei*

Department of Mechanical Engineering, Urmia University, 5756151818 Urmia, Iran

* Correspondence: Razieh Abbasgholi Rezaei (r_rezaei_mec@yahoo.com)

Received: 05-08-2023 **Revised:** 06-10-2023 **Accepted:** 06-27-2023

Citation: R. A. Rezaei, "Energy and exergy evaluation of a dual fuel combined cycle power plant: An optimization case study of the Khoy plant," *Power Eng. Eng. Thermophys.*, vol. 2, no. 2, pp. 97–109, 2023. https://doi.org/10.56578/peet020204.

Abstract: This study examines the energy and exergy performance of the Khoy dual fuel combined cycle power plant, focusing on dual pressure heat recovery steam generators (HRSGs). The aim is to identify an optimal design through the development of a thermodynamic model using ASPEN PLUS software. In the simulation, isentropic efficiencies of high-pressure and low-pressure steam turbines, gas turbines, and compressors are assumed to be 0.85, 0.80, 0.85, and 0.85, respectively. Various practical parameters, such as compressor pressure, condenser pressure, high-pressure steam turbine pressure, and outlet and inlet temperatures of superheaters and turbines, are investigated for their effects on energy and exergy efficiencies. The analysis reveals that combustion chamber I and combustion chamber II contribute the highest amounts of exergy destruction, accounting for 21.80% and 21.50% of the total exergy destruction, respectively. These areas are identified as requiring improvement. Based on the findings, an optimal design is presented, resulting in significant enhancements in energy and exergy efficiencies. The energy efficiency experiences a remarkable increase of 8.75%, while the exergy efficiency demonstrates a substantial improvement of 22.04%. This underscores the superiority of the optimized power plant configuration and provides valuable insights for designers, engineers, and power plant operators. In conclusion, this study advances the understanding of the energy and exergy performance of the Khoy dual fuel combined cycle power plant and offers guidance for optimizing its design and operation.

Keywords: Dual fuel; Combined cycle power plant; Heat recovery steam generators (HRSGs); Energy analysis; Exergy analysis; Efficiency; ASPEN PLUS

1 Introduction

In the current era, with limited energy resources, minimizing energy losses and enhancing efficiency have become critical topics for researchers. Combined cycle power plants (CCPPs) represent a well-established technology that offers improved thermal efficiency, increased power output, and reduced emissions compared to Brayton or Rankin cycles. The thermodynamic analysis of CCPPs necessitates the consideration of the first and second laws of thermodynamics. By applying the first law, energy quality can be measured through entropy analysis [1], while the second law enables the determination of both energy quality and quantity [2].

Srinivas et al. [3] investigated steam injection in a dual-pressure CCPP, while Fiaschi and Manfrida [4] conducted an exergy analysis to understand the primary origin of irreversibility in a gas turbine CCPP. Aljundi [5] carried out energy and exergy analyses in a steam power plant, and Ganapathy et al. [6] examined a lignite-fired power plant, identifying the combustor as the principal source of exergy losses. Cihan et al. [7] found that the combustion chambers produced the highest irreversibility in the Lüleburgaz power plant. Balli et al. [8] proposed an optimized exergy model for the Eskişehir power plant, while Woudstra et al. [9] applied thermodynamic evaluations to CCPPs, demonstrating that the highest losses were caused by fuel combustion. Reddy et al. [10] employed thermodynamic evaluations to analyze CCPPs with and without solar concentrators.

Kaviri et al. [11] performed comprehensive thermodynamic modeling and multi-objective optimization of a dual-pressure CCPP, revealing that the cost of exergy destruction in the combustion chamber exceeded that of other components, leading to the conclusion that increasing the gas turbine inlet temperature results in a decrease in the cost of exergy destruction. Ahmadi and Dincer [12] conducted exergy and exergy-economic analyses for a

CCPP, achieving an acceptable balance between thermodynamic and economic models by applying optimal design parameters. Kotowicz and Brzeczek [13] studied the net electric efficiency of a CCPP in the presence of steam cooling, indicating an improvement of 0.63–0.65 in net electric efficiency. Aliyu et al. [14] examined the impact of reheating equipment on a CCPP with triple pressure.

Although numerous studies have investigated CCPPs with a single fuel, research on dual fuel CCPPs remains scarce. The primary objective of this work is to analyze the effects of various practical parameters such as compressor pressure, condenser pressure, high-pressure steam turbine pressure, and outlet and inlet temperatures of superheaters and turbines on energy and exergy efficiencies. Furthermore, this study aims to propose an optimal design, simulated using ASPEN PLUS software, to enhance the performance of the dual fuel CCPP. It is essential to note that the optimized model represents a simulation rather than an actual implementation.

The remainder of this paper is organized as follows: Section 2 describes the system and simulation procedure; Section 3 presents the energy analysis; Section 4 provides the exergy analysis and calculates the exergy efficiency by considering exergy destruction for each component and the overall power plant; Section 5 discusses the results and their implications; and Section 6 concludes the study with key findings.

2 System Description

This study investigates the Khoy Combined Cycle Power Plant (CCPP) located in the northwest region of Iran. The Khoy CCPP operates as a combined cycle system, integrating the Brayton cycle for gas turbines and the Rankine cycle for steam turbines. The operational process commences with the compression of air in two compressors, followed by mixing with fuel, such as natural gas or gasoline, in the combustion chambers. The combustion reaction occurs at elevated temperatures, generating exhaust gases. These exhaust gases expand within the gas turbines, driving the compressors and generating excess work. The excess work is attributed to the temperature change in the airflow as it passes through the combustion chamber. The hot air-fuel mixture further expands through the gas turbine blades, causing the turbines to spin. The spinning gas turbines are connected to generators that convert the rotational energy into electricity. Simultaneously, the waste heat produced by the gas turbines is directed to heat exchangers within the Heat Recovery Steam Generators (HRSGs). The HRSGs utilize waste heat to generate steam at two distinct pressure levels. The steam produced in the HRSGs then enters both the high-pressure and low-pressure steam turbines, which are interconnected via a shared shaft. The steam turbines convert the thermal energy of the steam into rotational movement, which drives the generator shaft to generate electricity. Maximum efficiency is achieved by reducing the pressure and temperature of the steam as much as possible. This is accomplished by cooling the steam discharged from the low-pressure turbine, transforming it back into liquid water. Consequently, the condensed water from the condenser can be immediately reused as feed water, circulated by water pumps, and fed into the steam generators for the production of steam. This closed-loop system ensures efficient utilization of resources within the Khoy CCPP. Table 1 presents the actual operational data for the power plant, while Figure 1 depicts a schematic diagram showcasing the basic configuration of the dual-pressure combined cycle power plant in Khoy. The diagram illustrates the flow of energy within the system.

Table 1. Actual operational data for natural gas and gasoline-fired power plant of Khoy

	Natural gas section	**Gasoline section**
Gas turbine outlet pressure	1.1bar	1.1 bar
Gas turbine outlet temperature	542.9°C	543.6°C
HP superheater outlet pressure	85bar	85 bars
HP superheater heater outlet temperature	510°C	510°C
IP superheater outlet pressure	6.6bar	6.6bar
IP superheater outlet temperature	235°C	235°C
HP economizer inlet pressure	113.6 bar	105.6 bar
HP economizer inlet temperature	138.5°C	117°C
IP economizer inlet pressure	17.7 bar	16.6 bar
IP economizer inlet temperature	136.4°C	115.4°C
LP steam turbine inlet pressure of HP steam turbine	5.1bar	
LP steam turbine inlet temperature of HP steam turbine	174.5°C	
Condenser inlet temperature of LP steam turbine	49.9°C	
Condenser inlet pressure of LP steam turbine	0.1 bar	
Condenser inlet temperature	26.7°C	
Condenser inlet pressure	0.1bar	

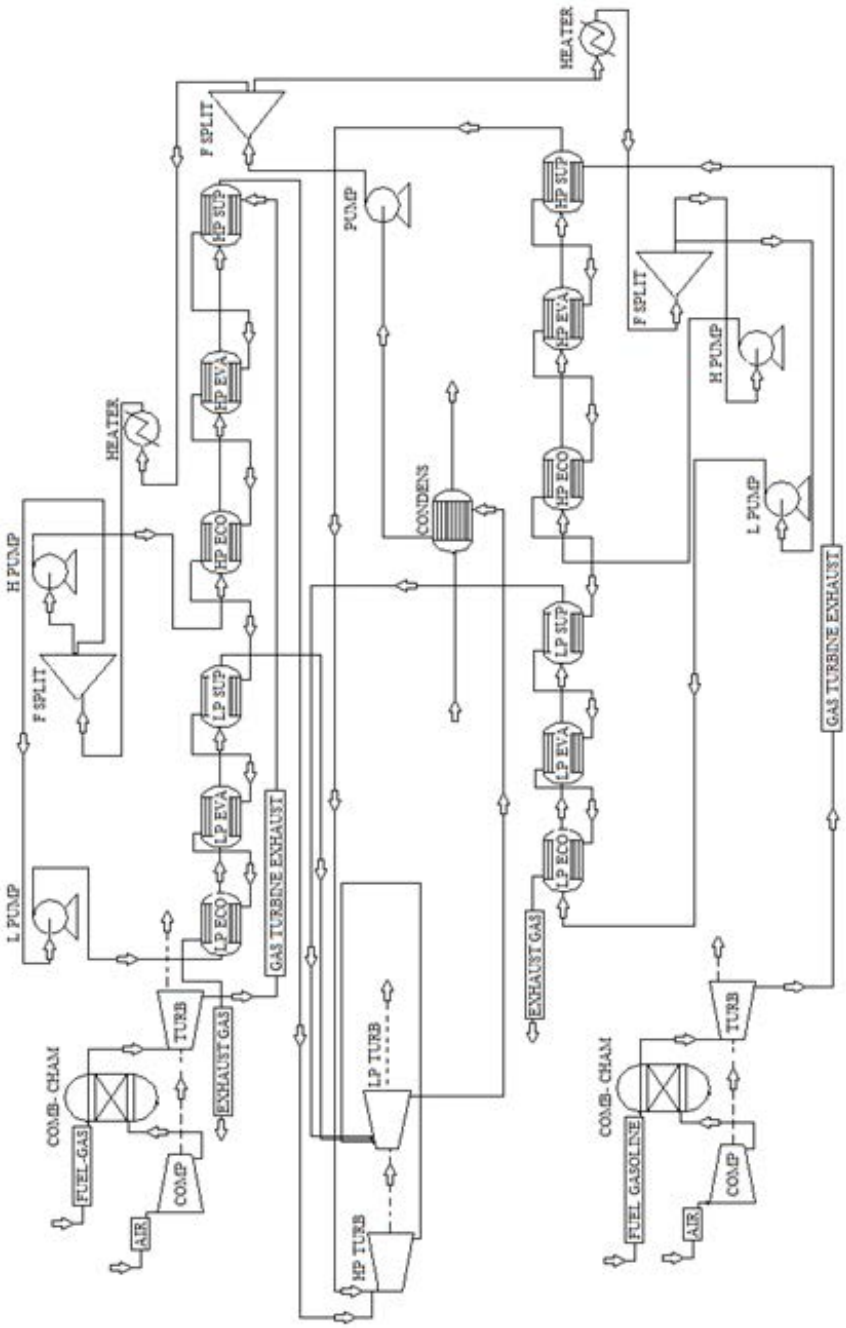

Figure 1. Schematic diagram of the dual-pressure combined cycle power plant in Khoy

2.1 ASPEN PLUS Modeling and Validation

The model of the CCPP is developed using ASPEN PLUS software. The physical property method employed in this simulation is RKS-BM (Redlich-Kwong-Soave-Boston-Mathias). Flow rate, composition, temperature, and pressure conditions for both fuels, natural gas and gasoline, are provided in Table 2. Natural gas comprises a combination of multiple hydrocarbons. For simplicity, natural gas is considered as a mixture of methane, ethane, nitrogen, and carbon dioxide in this study. The plant design is based on T = 15℃ and P = 1.01 bar for the air inlet stream. Although these conditions may vary for a plant in different seasons, an average environmental condition has been employed in this study.

Several assumptions have been made for simulating the CCPP using ASPEN PLUS software, which are presented in Table 3. To verify the simulation results, the power generation of natural gas and gasoline sections, as well as the work produced from the high-pressure (HP) and low-pressure (LP) turbines of the simulated power plant, were compared with the actual data of the Khoy power plant. The results demonstrate good agreement, as shown in

Table 4.

Table 2. Fuels composition and conditions

Composition and conditions of natural gas	
N_2	0.022
CO_2	0.022
CH_4	0.940
C_2H_6	0.033
Vapor fraction	1
Temperature [°C]	18
Pressure [bar]	22
Mass flow [kg/s]	10
Composition and conditions of gasoline	
N-DODECANE	1
Vapor fraction	0
Temperature [°C]	15
Pressure [bar]	1.010
Volumetric flow rate[lit/hr]	34000

Table 3. Assumptions made for the simulation of CCPP using ASPEN PLUS software

Parameter	**Assumed amount**
Combustion chambers heat duty	0
Turbines heat duty	0
Compressors heat duty	0
Pumps heat duty	0
Condensers heat duty	0
High-pressure steam turbine isentropic efficiency	0.85
Low-pressure steam turbine isentropic efficiency	0.80
Gas turbines isentropic efficiencies	0.85
Compressors isentropic efficiencies	0.85

Table 4. Comparison of power generation of the simulated power plant with the actual one

	Natural gas section power generation (MW)	**Gasoline section power generation (MW)**	**HP turbine work (MW)**	**LP turbine work (MW)**
Simulation	191.54	201.94	51.22	101.6
Actual data	190	200	50	99.5

3 Thermodynamics Analysis

3.1 Energy Analysis

The first law of thermodynamics in an open flow system, where there are three types of energy transfer including work, heat, and energy-related to mass transfer in the control surface under a steady-state condition, is presented as follows [15],

$$\sum \dot{Q} + \dot{m}\left(h_i + \frac{c_i^2}{2} + gZ_i\right) = \dot{m}\left(h_o + \frac{c_o^2}{2} + gZ_o\right) + \dot{W} \tag{1}$$

where, $\dot{Q}, \dot{m}, C, g, Z, h$, and $\dot{W}$ stand for the rate of heat input to the system [MW], mass flow rate $[kgs^{-1}]$, velocity [m/s], gravity $\left[m/s^2\right]$, height [m], specific enthalpy $\left[kJ\,kg^{-1}\right]$, and the rate of work produced by the system [MW], respectively.

3.1.1 Energy efficiency

The efficiency of a system, known as the energetic or first law efficiency (η_I), is determined by the ratio of the system's output energy to its input energy. This measurement indicates the effectiveness of converting input energy into useful output energy within the system.

$$\eta_{\mathrm{I}} = \frac{\text{Desired output energy}}{\text{Input energy supplied}} = \frac{\sum \dot{\mathrm{W}}_{\text{net}}}{\sum \dot{\mathrm{Q}}_{in}}. \tag{2}$$

The output and input energies can be in turn defined as

$$\sum \dot{\mathrm{W}}_{\text{net}} = \dot{\mathrm{W}}_{\mathrm{GTI}} + \dot{\mathrm{W}}_{\mathrm{GT\,II}} + \dot{\mathrm{W}}_{\mathrm{ST}} - \dot{\mathrm{W}}_{\text{comp I}} - \dot{\mathrm{W}}_{\text{comp II}} - \sum \dot{\mathrm{W}}_{\text{pump}} \tag{3}$$

$$\sum \dot{\mathrm{Q}}_{\mathrm{in}} = [\dot{\mathrm{m}}\,(\mathrm{h_o} - \mathrm{h_i})]_{\text{comb1}} + [\dot{\mathrm{m}}\,(\mathrm{h_o} - \mathrm{h_i})]_{\text{comb2}} \tag{4}$$

Note that subscripts I and II denote natural gas fired cycle and gasoline fired cycle, respectively. In Eq. (3), pumps work is negligible in comparison to the other parameters.

3.2 Exergy Analysis

The exergy of a thermal system is the maximum work that can be obtained from the system, and any irreversibilities within the system result in the destruction of exergy . The equation for exergy in an open system operating under steady-state conditions is provided as: [16, 17],

$$\sum_{\mathrm{j}} \left(1 - \frac{\mathrm{T_i}}{\mathrm{T_o}}\right) \dot{\mathrm{Q}}_{\mathrm{j}} - \dot{\mathrm{W}}_{\mathrm{cv}} + \sum_{\mathrm{i}} \dot{\mathrm{m}}_{\mathrm{i}} \varepsilon_{\mathrm{i}} - \sum_{\mathrm{e}} \dot{\mathrm{m}}_{\mathrm{e}} \varepsilon_{\mathrm{e}} - \dot{\mathrm{E}}_{\mathrm{D}} = 0 \tag{5}$$

where, $\mathrm{T_i}, \mathrm{T_0}, \dot{\mathrm{Q}}, \dot{\mathrm{W}}_{\mathrm{cv}}, \dot{\mathrm{m}}_{\mathrm{i}}, \dot{\mathrm{m}}_{\mathrm{e}}, \mathcal{E}_{\mathrm{i}}, \mathcal{E}_{\mathrm{e}}$, and $\dot{\mathrm{E}}_{\mathrm{D}}$ are inlet temperature, outlet temperature, the rate of heat input to the system [MW], the rate of work produced in control volume [MW], inlet mass flow rate $\left[\mathrm{kgs}^{-1}\right]$, outlet mass flow rate $\left[\mathrm{kgs}^{-1}\right]$, inlet specific exergy $\left[\mathrm{kJkg}^{-1}\right]$, outlet specific exergy $\left[\mathrm{kJkg}^{-1}\right]$, and Time rate of exergy destruction [MW].

By rearranging Eq. (5), we obtain the exergy destruction of a control volume in a steady-state open system.

$$\dot{\mathrm{E}}_{\mathrm{D}} = \sum_{\mathrm{j}} \dot{\mathrm{E}}_{\mathrm{Qj}} \dot{\mathrm{Q}}_{\mathrm{j}} - \dot{\mathrm{W}}_{\mathrm{cv}} + \sum_{\mathrm{i}} \dot{\mathrm{m}}_{\mathrm{i}} \varepsilon_{\mathrm{i}} - \sum_{\mathrm{e}} \dot{\mathrm{m}}_{\mathrm{e}} \varepsilon_{\mathrm{e}} \tag{6}$$

When nuclear, magnetic, electrical, and surface tension effects are not present, the total exergy of a system can be categorized into four components: physical $(\dot{E}_{PH})$, chemical $(\dot{E}_{\mathrm{CH}})$, potential $(\dot{E}_{\mathrm{PT}})$ and kinetic exergy $(\dot{E}_{\mathrm{KN}})$.

$$\dot{\mathrm{E}}_{\text{total}} = \dot{\mathrm{E}}_{\mathrm{PH}} + \dot{\mathrm{E}}_{\mathrm{CH}} + \dot{\mathrm{E}}_{\mathrm{PT}} + \dot{\mathrm{E}}_{\mathrm{KN}} \tag{7}$$

By disregarding potential and kinetic exergies, the following relation can be obtained for total exergy,

$$\dot{\mathrm{E}}_{\text{total}} = \dot{\mathrm{E}}_{\mathrm{PH}} + \dot{\mathrm{E}}_{\mathrm{CH}} \tag{8}$$

The specific physical exergy can be represented by the following expression:

$$\dot{\mathrm{E}}_{\mathrm{PH}} = \dot{\mathrm{m}}\,[(\mathrm{h} - \mathrm{h_0}) - \mathrm{T_0}\,(\,\mathrm{s} - \mathrm{s_0})] \tag{9}$$

Therefore,

$$\dot{\mathrm{E}}_{\text{total}} = \dot{\mathrm{m}}\,[(\mathrm{h} - \mathrm{h_0}) - \mathrm{T_0}\,(\,\mathrm{s} - \mathrm{s_0})] + \dot{\mathrm{E}}_{\mathrm{CH}} \tag{10}$$

where, the subscript "0" denotes reference conditions.

To evaluate the chemical exergy for mixtures containing gases not listed in the reference tables, the following equation can be utilized: [18, 19],

$$\mathcal{E}_{\mathrm{CH}} = \sum \mathrm{x_n} \left(\mathcal{E}_{\mathrm{CH}}\right)_{\mathrm{n}} + \mathrm{RT_0} \sum \mathrm{x_n} \ln \mathrm{x_n} \tag{11}$$

Here, $\mathrm{X_n}$ is the mole fraction of the $\mathrm{k_{th}}$ gas in the mixture, and R is the universal gas constant. In exergy analysis, another crucial factor that must be taken into account is the reference conditions. For this study, the reference conditions are defined as the atmospheric temperature of 15℃ and pressure of 1.01 bar. The above equation (Eq. (11)) cannot be utilized for evaluating the fuel exergy [20–22],

$$\xi = \frac{\varepsilon_{CH,fuel}}{LHV_{\mathrm{fuel}}} \tag{12}$$

The lower heating value (LHV), referred to as the net calorific value, of a fuel is determined by combusting a specified quantity of the fuel (initially at 25℃) and restoring the temperature of the combustion products to 150℃. In the case of gaseous fuels with a composition of $\mathrm{C_xH_y}$, a specific experimental equation is employed to calculate the parameter ξ, representing the fuel exergy [21],

$$\xi = 1.033 + 0.0169\frac{\mathrm{y}}{\mathrm{x}} - \frac{0.0698}{\mathrm{x}} \tag{13}$$

For liquid fuel with $\mathrm{C_xH_y}$, the following experimental equation is used to calculate ξ [21]:

$$\xi = 1.04224 + 0.011925\frac{\mathrm{y}}{\mathrm{x}} - \frac{0.042}{\mathrm{x}} \tag{14}$$

3.2.1 Exergy efficiency

The exergy or second law efficiency is defined as the ratio or measure of the actual useful work or output obtained from a system to the maximum possible work or output that can be obtained from the same system under the given operating conditions.

$$\eta_{\mathrm{II}} = \frac{\text{Actual thermal efficiency}}{\text{possible (reversible) thermal efficiency}} = \frac{\text{Exergy output}}{\text{Exergy input}} = 1 - \frac{\text{Exergy Loss}}{\text{Exergy Input}} \tag{15}$$

3.2.2 Component-wise exergy analysis

According to Eq. (6), the exergy equations for each component, assumed as a control volume, can be calculated. The exergy destruction equations and exergy efficiencies for various parts of the CCPP are as follows:

• Air compressor

$$\dot{\mathrm{E}}_{\mathrm{D,\,Comp}} = \dot{\mathrm{m}}_{\mathrm{air}} \left(\varepsilon_{\mathrm{in}} - \varepsilon_{\mathrm{out}}\right) + \dot{\mathrm{W}}_{\mathrm{Comp}} \tag{16}$$

$$\eta_{\mathrm{II,Comp}} = \frac{\dot{\mathrm{m}}_{\mathrm{air}} \left(\mathcal{E}_{\mathrm{out}} - \mathcal{E}_{\mathrm{in}}\right)}{\dot{\mathrm{w}}_{\mathrm{Comp}}} \tag{17}$$

• Combustion chamber

$$\dot{\mathrm{E}}_{\mathrm{D,Comb}} = \dot{\mathrm{m}}_{\mathrm{air}}\, \varepsilon_{\mathrm{air}} + \dot{\mathrm{m}}_{\mathrm{fuel}}\, \varepsilon_{\mathrm{fuel}} - \dot{\mathrm{m}}_{\mathrm{pro}}\, \varepsilon_{\mathrm{pro}} \tag{18}$$

$$\mathrm{n_{II,Comb}} = 1 - \frac{\dot{\mathrm{E}}_{\mathrm{D\ Comb}}}{\dot{\mathrm{m}}_{\mathrm{air}}\, \varepsilon_{\mathrm{air}} + \dot{\mathrm{m}}_{\mathrm{fuel}}\, \varepsilon_{\mathrm{fuel}}} \tag{19}$$

• Gas turbine

$$\dot{E}_{D,GT} = \dot{m}_{pro}\ (\varepsilon_{in}\ - \varepsilon_{out}\ ) - \dot{W}_{GT} \tag{20}$$

$$\eta_{II,GT} = \frac{\dot{W}_{GT}}{\dot{m}_{pro}\ (\varepsilon_{in} - \varepsilon_{out}\ )} \tag{21}$$

• Heat recovery steam generator

$$\dot{E}_{D,HRSG} = \dot{m}_{g}\ (\varepsilon_{gin}\ - \varepsilon_{gout}\ ) + \dot{m}_{w}\ (\varepsilon_{win}\ - \varepsilon_{wout}\ ) \tag{22}$$

$$\eta_{II,HRSG} = \frac{\dot{m}_{w}\ (\mathcal{E}_{wout} - \mathcal{E}_{win}\ )}{\dot{m}_{g}\ (\mathcal{E}_{gout} - \mathcal{E}_{gin}\ )} \tag{23}$$

• Steam turbine

$$\dot{E}_{D,ST} = \dot{m}_{pro}\ (\varepsilon_{in}\ - \varepsilon_{out}\ ) - \dot{W}_{ST} \tag{24}$$

$$\eta_{II,ST} = \frac{\dot{W}_{ST}}{\dot{m}_{pro}\ (\varepsilon_{in}\ - \varepsilon_{out}\ )} \tag{25}$$

• Condenser

$$\dot{E}_{D,\ Cond}\ = \dot{m}_{pro}\ (\mathcal{E}_{in}\ - \mathcal{E}_{out}\ ) \tag{26}$$

$$\eta_{II,\ Cond}\ = 1 - \frac{\dot{E}_{D\ Cond}}{\dot{m}_{in}\mathcal{E}_{in}} \tag{27}$$

• Combined cycle power plant

$$\dot{E}_{D,CCPP} = \dot{E}_{DComp} + \dot{E}_{DComb} + \dot{E}_{DGT} + \dot{E}_{DST} + \dot{E}_{DHRSG} + \dot{E}_{DCond} \tag{28}$$

$$\eta_{II,CCPP}\ = \frac{\dot{W}_{net}}{\dot{E}_{in}\ - \dot{E}_{out}} \tag{29}$$

$$\dot{E}_{in} = \dot{m}_{fuel}\ \mathcal{E}_{fuel}\ + \dot{m}_{air}\ \mathcal{E}_{air} \tag{30}$$

$$\dot{E}_{out}\ = \dot{m}_{pro}\ \mathcal{E}_{out\ HRSG} \tag{31}$$

4 Results and Discussion

4.1 Effects of Gas Turbine Inlet Temperature and Compressor Pressure Ratio

The performance of a combined cycle is significantly influenced by the inlet temperature of the gas turbine, as it directly affects the power output of the turbine. To investigate the effect of gas turbine inlet temperature, power generation of the CCPP was calculated at three different gas turbine inlet temperatures: 1200℃, 1300℃, and 1400℃. The results are depicted in Figure 2. The production of additional electricity necessitates an increase in the inlet

temperature of gas turbines, which is dependent on the compressor pressure ratio. Therefore, this parameter plays a crucial role in determining the performance of the combined cycle [23].

For each gas turbine inlet temperature considered in this section, the effect of the compressor pressure ratio on the CCPP power generation was investigated, as shown in Figure 2. It was observed that, for a specific gas turbine inlet temperature, the power produced initially increased with the pressure ratio to a maximum value and then tended to decrease. Compressor pressure ratios at gas turbine inlet temperatures of 1200, 1300, and 1400℃ varied within the applicable ranges of 10-17, 10-20, and 10-22, respectively. The maximum desirable compressor pressure ratios for gas turbine inlet temperatures of 1200℃, 1300℃, and 1400℃ were found to be 14, 16, and 19, respectively, as indicated by the black points in Figure 2. It should be noted that the gas turbine inlet temperature should not exceed 1400℃ (the maximum allowable operating temperature of the turbine components) due to material temperature limitations, and the compressor pressure ratio must not exceed 22 because of commercial availability [23]. It can be concluded that the maximum power generation occurred at a gas turbine inlet temperature of 1400℃ and a compressor pressure ratio of 19.

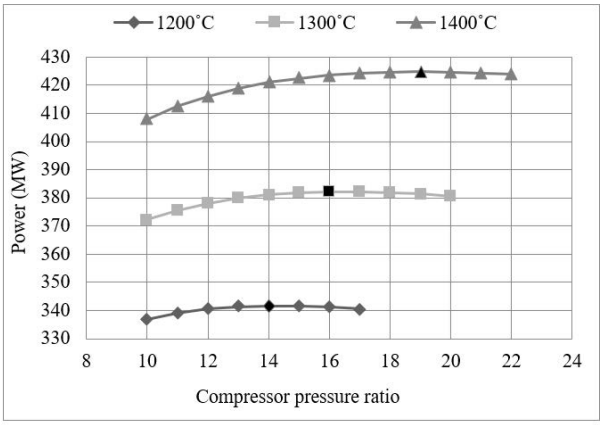

Figure 2. Effects of gas turbine inlet temperatures and compressor pressure ratio on the CCPP power generation

4.2 Effect of High-Pressure Heat Recovery Steam Generator (HP HRSG) Working Pressure

Alterations in the outlet stream pressure of HP HRSGs could affect the power plant efficiency. The outlet pressure of HP HRSGs was varied from 85 to 120 bar. However, the gas turbine's inlet temperature and compressor pressure ratio were held constant at 1400℃ and 19, respectively. The results are shown in Figure 3. It was evident that an increase in the pressure of the HP HRSG resulted in an increase in power generation [24]. This increase was sharp initially, and then further increasing the HP HRSG pressure had little effect on the power generation. Due to commercial limitations, the HP HRSG outlet pressure was limited to 120 bar.

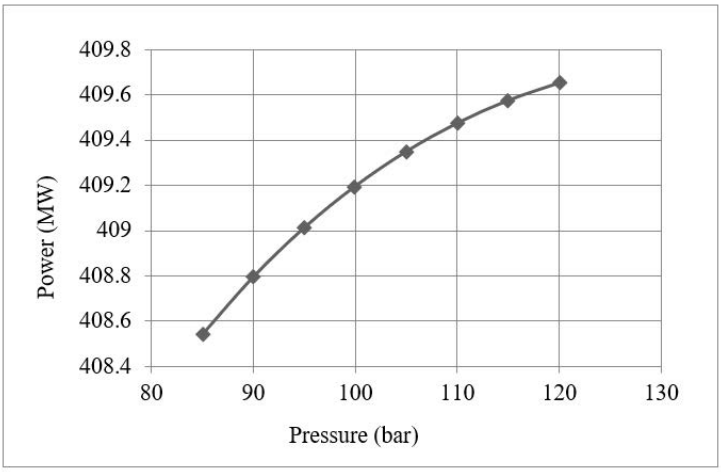

Figure 3. Effect of working pressure of HP HRSGs on the performance of CCPP at gas turbine inlet temperature of 1400℃ and compressor pressure ratio of 19

4.3 Effect of Low-Pressure (LP) and High-Pressure (HP) Superheater Outlet Temperatures

To examine the effect of LP and HP superheater outlet temperatures on the power generation of the CCPP, the outlet temperatures of LP and HP superheaters were varied from 235℃ to 300℃ (Figure 4) and 510℃ to 620℃ (Figure 5), respectively. As can be seen from these figures, an increase in superheater outlet temperature led to increased power generation. An increase of 20℃ in temperature resulted in an increase of approximately 215 kW in the LP section and about 2300 kW in the HP section. It appeared that the HP outlet temperature had a greater effect on CCPP performance than the LP outlet temperature. The outlet streams of HP and LP superheaters were led to the LP and HP steam turbines. Increasing the steam temperature meant less erosion in the final stages of the steam turbines, but due to metallurgical constraints, these temperatures should not exceed 300℃ and 620℃, respectively, for LP and HP steam turbines [25].

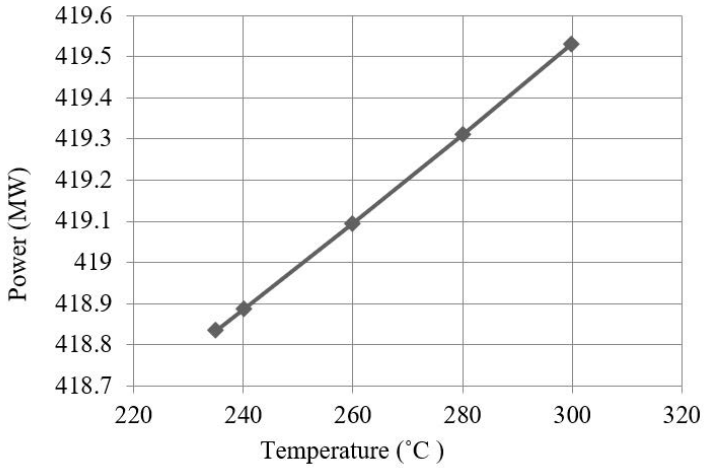

Figure 4. Effect of LP superheater outlet temperature on the performance of CCPP at gas turbine inlet temperature of 1400℃ and compressor pressure ratio of 19

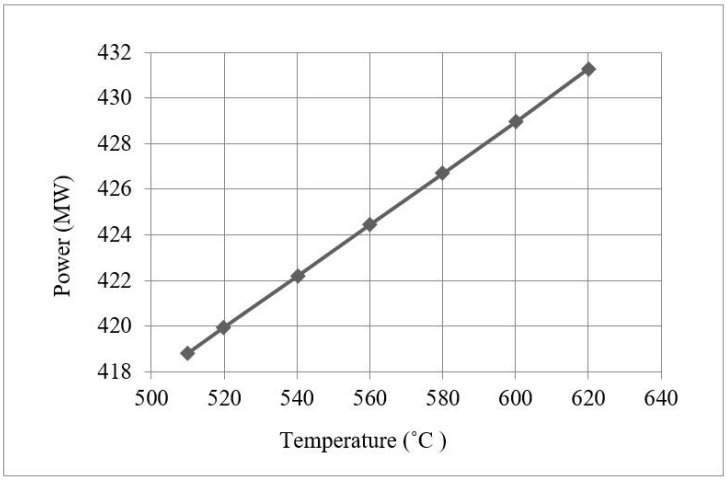

Figure 5. Effect of HP superheater outlet temperature on the performance of CCPP at gas turbine inlet temperature of 1400℃ and compressor pressure ratio of 19

4.4 Effect of Condenser Working Pressure

The impact of condenser working pressure on the power generation of the CCPP is illustrated in Figure 6. A decrease in condenser pressure was found to result in an increase in power generation. In this analysis, condenser pressure was varied from 0.1 to 0.25 bar, with the maximum power generation occurring at a condenser pressure of 0.1 bar. Consequently, selecting a lower condensing head pressure was identified as a highly effective method for enhancing CCPP performance. However, the condenser pressure could not be reduced below 0.1 bar due to limitations in the damp fraction at the steam turbine outlet [26].

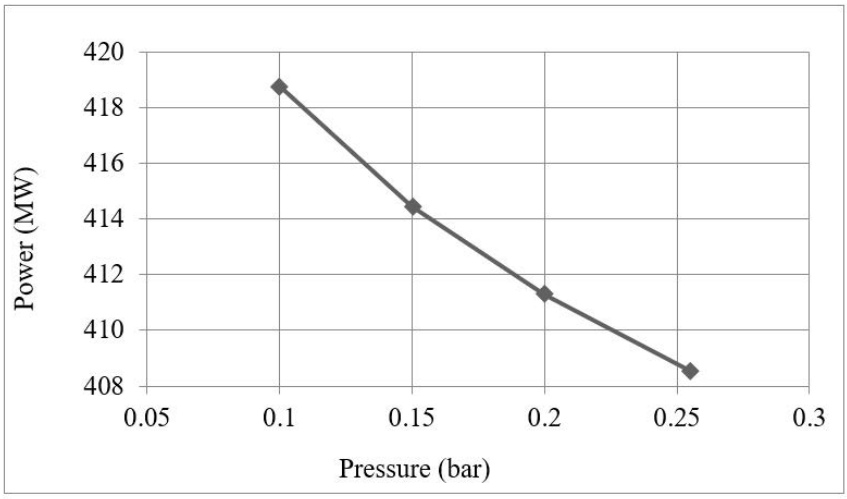

Figure 6. Effect of condenser working pressure on CCPP performance at gas turbine inlet temperature of 1400°C and compressor pressure ratio of 19

4.5 Energy Loss and Efficiency

Energy losses for each component of the original Khoy power plant and the optimized model are presented in Figures 7 and 8, respectively. The optimized model was obtained by applying conditions that resulted in the highest power generation, as determined from the energy analysis in Sections 4.2 through 4.5 (as shown in Figures 3- 6). According to the first law analysis, gas turbines exhibited the most significant energy loss in both the original and optimized power plant models. Using Eq. (2), the first law efficiency, η_I, was calculated to be 54.65% for the original power plant and 63.4% for the optimized model, indicating an increase of 8.75% in energy efficiency.

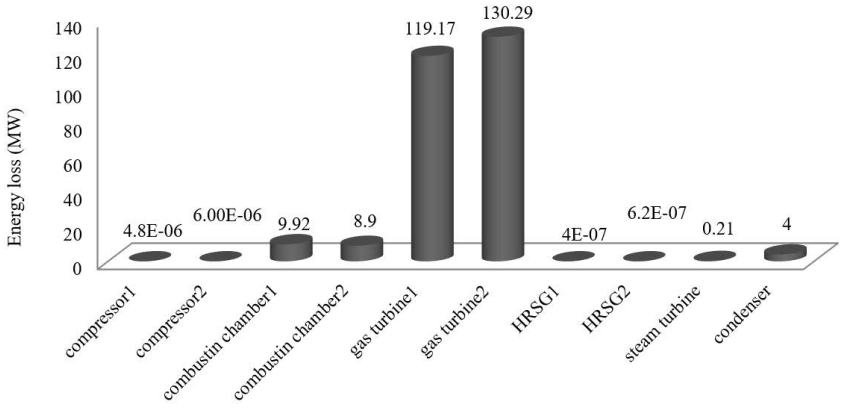

Figure 7. Energy loss of the original Khoy power plant components

4.6 Exergy Loss and Efficiency

Optimal design for the Khoy power plant, from an energy perspective, was achieved by conducting an energy analysis and determining the effect of adjustable parameters. In this section, calculations were performed to determine the exergy efficiencies and losses of the optimized power plant components. The aim was to identify critical components within the system that require improvement. Table 5 presents the exergy destruction and exergy efficiency data for the optimized power plant components.

The maximum exergy destruction was observed in combustion chamber I and combustion chamber II, accounting for 21.80% and 21.50% of total exergy destruction, respectively. As per the data provided in Table 5, chemical reactions contributed to a significant portion of exergy destruction compared to heat transfer and friction. However, based on the first law analysis, gas turbines were identified as the primary source of energy loss within the system (refer to Section 4.5). This finding suggests that the first law analysis alone is insufficient for determining the main source of power loss (exergy destruction).

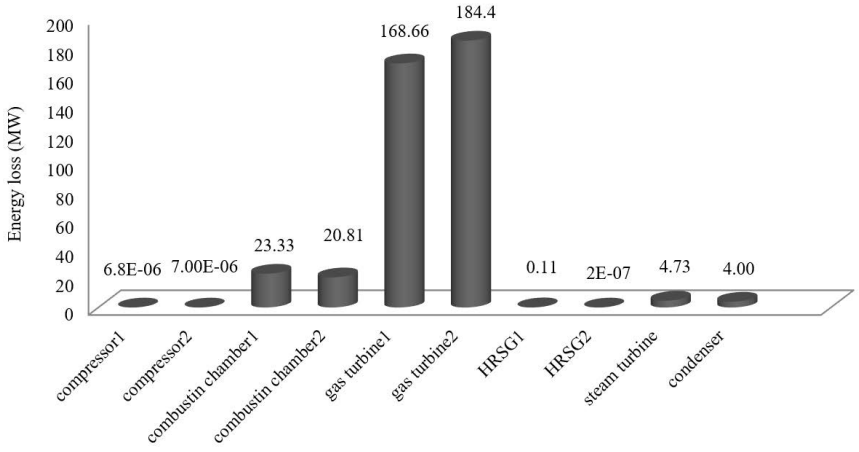

Figure 8. Energy loss of the optimized model components

Gas turbine I, gas turbine II, and the steam turbine, with exergy destructions of 14.77%, 16.15%, and 15.09%, respectively, were the subsequent most significant components requiring improvement. The total exergy destruction for the optimized power plant was 1264 MW. Table 5 reveals that compressor I, compressor II, combustion chamber I, and combustion chamber II exhibited high exergy efficiencies of 93.71%, 93.1%, 94.93%, and 95.39%, respectively. In contrast, the steam turbine, gas turbine I, gas turbine II, and condenser had low exergy efficiencies of $34.28\%, 44.95\%, 44.98\%$, and 47.25%, respectively. Using Eq. (29), the exergy efficiency for the original Khoy power plant and the optimized model were calculated as 47.19% and 69.23%, demonstrating a 22.04% improvement in exergy efficiency.

Table 5. The optimized power plant's exergy destruction data and exergy efficiency at different points throughout the plant

Components	**Exergy destruction** [**M W**]	**Percent exergy destruction** [**%**]	**Exergy efficiency** [**%**]
Compressor I	10.61	0.84	93.71
Compressor II	11.6	0.92	93.71
Combustion chamber I	275.57	21.8	94.93
Combustion chamber II	271.86	21.5	95.39
Gas turbine I	186.74	14.77	44.95
Gas turbine II	204.13	16.15	44.98
HRSG I	47.16	3.73	51.38
HRSG II	52.14	4.12	49.3
Steam turbine	190.75	15.09	34.28
Condenser	13.75	1.09	47.25

5 Conclusions

In this study, a dual-fuel combined cycle power plant, employing both gas and gasoline, was modeled and optimized utilizing ASPEN PLUS software. The simulation results were validated by comparing them with actual data from the existing plant, demonstrating a satisfactory agreement. An energy and exergy analysis was performed on the combined cycle power plant, focusing on both the gas (Brayton cycle) and steam (Rankine cycle) sections. Optimal design parameters were determined through this analysis.

For the gas section, it was discovered that maximum power generation could be attained with a gas turbine inlet temperature of 1400°C and a compressor pressure ratio of 19. In the steam section, optimal values were identified as 120 bar for the inlet pressure of the high-pressure steam turbine, 300°C for the outlet temperature of the low-pressure heat recovery steam generator (HRSG), and 620°C for the outlet temperature of the high-pressure HRSG. Moreover, a condenser working pressure of 0.1 bar was deemed the optimum value.

An exergy analysis of the optimized model was conducted to evaluate the exergy efficiencies and exergy losses in all components of the power plant. This analysis revealed that combustion chamber I and combustion chamber II exhibited the highest exergy destruction, accounting for 21.80% and 21.50% of the total exergy destruction, respectively. These results highlight the components requiring improvement for optimization purposes.

Significant enhancements in both energy and exergy efficiencies were observed for the Khoy power plant upon implementing the optimized design. Energy efficiency increased by 8.75%, while exergy efficiency experienced a substantial improvement of 22.04%. These advancements demonstrate the superiority of the optimized power plant configuration over the existing one. The findings of this study provide valuable insights and guidance for designers, engineers, and power plant operators in their pursuit of improved performance and efficiency.

Data Availability

The data used to support the findings of this study are available from the corresponding author upon request.

Conflicts of Interest

The author declares no conflict of interest.

References

[1] M. Belli and E. Sciubba, "An application of the extended exergy accounting method to the analysis of an academic institution," *Proc. ECOS*, vol. 1, 2001.

[2] V. Nikulshin, C. Wu, and V. Nikulshina, "Exergy efficiency calculation of energy intensive systems," *Exergy Int. J.*, vol. 2, no. 2, pp. 78–86, 2002. https://doi.org/10.1016/S1164-0235(01)00042-5

[3] T. Srinivas, A. V. S. S. K. S. Gupta, and B. V. Reddy, "Sensitivity analysis of stig based combined cycle with dual pressure HRSG," *Int. J. Therm. Sci.*, vol. 47, no. 9, pp. 1226–1234, 2008. https://doi.org/10.1016/j.ijthermalsci.2007.10.002

[4] D. Fiaschi and G. Manfrida, "Exergy analysis of the semi-closed gas turbine combined cycle (SCGT/CC)," *Energy Convers. Manag.*, vol. 39, no. 16-18, pp. 1643–1652, 1998. https://doi.org/10.1016/S0196-8904(98)00067-3

[5] I. H. Aljundi, "Energy and exergy analysis of a steam power plant in Jordan," *Appl. Therm. Eng.*, vol. 29, no. 2-3, pp. 324–328, 2009.

[6] T. Ganapathy, N. Alagumurthi, R. P. Gakkhar, and K. Murugesan, "Exergy analysis of operating lignite fired thermal power plant," *J. Eng. Sci. Technol. Rev.*, vol. 2, no. 1, pp. 123–130, 2009.

[7] A. Cihan, O. Hacıhafızog˘lu, and K. Kahveci, "Energy–exergy analysis and modernization suggestions for a combined-cycle power plant," *Int. J. Energy Res.*, vol. 30, no. 2, pp. 115–126, 2006. https://doi.org/10.1002/er.1133

[8] O. Balli, H. Aras, and A. Hepbasli, "Exergetic performance evaluation of a combined heat and power (CHP) system in Turkey," *Int. J. Energy Res.*, vol. 31, no. 9, pp. 849–866, 2007. https://doi.org/10.1002/er.1270

[9] N. Woudstra, T. Woudstra, A. Pirone, and T. Van Der Stelt, "Thermodynamic evaluation of combined cycle plants," *Energy Convers. Manag.*, vol. 51, no. 5, pp. 1099–1110, 2010. https://doi.org/10.1016/j.enconman.2009.12.016

[10] V. S. Reddy, S. C. Kaushik, and S. K. Tyagi, "Exergetic analysis of solar concentrator aided natural gas fired combined cycle power plant," *Renew. Energy*, vol. 39, no. 1, pp. 114–125, 2012. https://doi.org/10.1016/j.renene.2011.07.031

[11] A. G. Kaviri, M. N. M. Jaafar, and T. M. Lazim, "Modeling and multi-objective exergy based optimization of a combined cycle power plant using a genetic algorithm," *Energy Convers. Manag.*, vol. 58, pp. 94–103, 2012. https://doi.org/10.1016/j.enconman.2012.01.002

[12] P. Ahmadi and I. Dincer, "Thermodynamic analysis and thermoeconomic optimization of a dual pressure combined cycle power plant with a supplementary firing unit," *Energy Convers. Manag.*, vol. 52, no. 5, pp. 2296–2308, 2011. https://doi.org/10.1016/j.enconman.2010.12.023

[13] J. Kotowicz and M. Brzeczek, "Analysis of increasing efficiency of modern combined cycle power plant: A case study," *Energy*, vol. 153, pp. 90–99, 2018. https://doi.org/10.1016/j.energy.2018.04.030

[14] M. Aliyu, A. B. AlQudaihi, S. A. Said, and M. A. Habib, "Energy, exergy and parametric analysis of a combined cycle power plant," *Therm. Sci. Eng. Prog.*, vol. 15, p. 100450, 2020. https://doi.org/10.1016/j.tsep.2019.100450

[15] V. Chauhan, P. A. Kishan, and S. Gedupudi, "Thermodynamic analysis of a combined cycle for cold storage and power generation using geothermal heat source," *Therm. Sci. Eng. Prog.*, vol. 11, pp. 19–27, 2019. https://doi.org/10.1016/j.tsep.2019.03.009

[16] V. G. Gude, "Use of exergy tools in renewable energy driven desalination systems," *Therm. Sci. Eng. Prog.*, vol. 8, pp. 154–170, 2018. https://doi.org/10.1016/j.tsep.2018.08.012

[17] E. Bellos and C. Tzivanidis, "Energetic and exergetic evaluation of a novel trigeneration system driven by parabolic trough solar collectors," *Therm. Sci. Eng. Prog.*, vol. 6, pp. 41–47, 2018. https://doi.org/10.1016/j.tsep.2018.03.008

[18] P. Ahmadi and I. Dincer, "Exergoenvironmental analysis and optimization of a cogeneration plant system using Multimodal Genetic Algorithm (MGA)," *Energy*, vol. 35, no. 12, pp. 5161–5172, 2010. https://doi.org/10.1016/j.energy.2010.07.050

[19] V. S. Reddy, S. C. Kaushik, and S. K. Tyagi, "Exergetic analysis of solar concentrator aided natural gas fired combined cycle power plant," *Renew. Energy*, vol. 39, no. 1, pp. 114–125, 2012. https://doi.org/10.1016/j.renene.2011.07.031

[20] J. Szargut, D. R. Morris, and F. R. Steward, *Exergy Analysis of Thermal, Chemical, and Metallurgical Processes*. New York: Hemisphere, 1987.

[21] M. R. Meigounpoory, P. Ahmadi, A. R. Ghaffarizadeh, and S. Khanmohammadi, "Optimization of combined cycle power plant using sequential quadratic programming," in *Proc. Heat Transfer Summer Conf.*, Florida, USA: ASME, 2008, pp. 109–114.

[22] M. Ameri, P. Ahmadi, and S. Khanmohammadi, "Exergy analysis of a 420 MW combined cycle power plant," *Int. J. Energy Res.*, vol. 32, no. 2, pp. 175–183, 2008. https://doi.org/10.1002/er.1351

[23] T. K. Ibrahim and M. M. Rahman, "Effect of compression ratio on performance of combined cycle gas turbine," *Int. J. Energy Eng.*, vol. 2, no. 1, pp. 9–14, 2012. https://doi.org/10.5923/j.ijee.20120201.02

[24] H. Hajabdollahi, P. Ahmadi, and I. Dincer, "An exergy-based multi-objective optimization of a heat recovery steam generator (HRSG) in a combined cycle power plant (CCPP) using evolutionary algorithm," *Int. J. Green Energy*, vol. 8, no. 1, pp. 44–64, 2011. https://doi.org/10.1080/15435075.2010.529779

[25] M. I. Riady, D. Santoso, and M. D. Bustan, "Thermodynamics performance evaluation in combined cycle power plant by using combined pinch and exergy analysis," *J. Phys.: Conf. Ser.*, vol. 1198, no. 4, p. 042006, 2019. https://doi.org/10.1088/1742-6596/1198/4/042006

[26] C. C. Chuang and D. C. Sue, "Performance effects of combined cycle power plant with variable condenser pressure and loading," *Energy*, vol. 30, no. 10, pp. 1793–1801, 2005. https://doi.org/10.1016/j.energy.2004.10.003

Nomenclature

h	Specific enthalpy $\left[\mathrm{kJkg}^{-1}\right]$
$\dot{\mathrm{Q}}$	Heat loss flow rate $[\mathrm{MW}]$
s	Specific entropy $\left[\mathrm{kJkg}^{-1}\ \mathrm{K}^{-1}\right]$
P	Pressure [bar]
$\dot{\mathrm{m}}$	Mass flow rate $\left[\mathrm{kgs}^{-1}\right]$
$\dot{\mathrm{E}}$	Exergy rate $[\mathrm{MW}]$
$\dot{\mathrm{W}}$	Power $[\mathrm{MW}]$
T	Temperature $[^{\circ}\mathrm{C}]$

Subscripts

comp	Compressor
comb	Combustion chamber
cond	Condenser
e	Exit
CH	Chemical
CCPP	Combined cycle power plant
GT	Gas turbine
ST	Steam turbine
PH	Physical
CV	Control volume
0	Dead state condition
LP	Low pressure
HP	High pressure
KN	Kinetic
PT	Potential
D	Destruction
Pro	Product

Greek symbols

ε	Specific exergy $\left[\mathrm{kJkg}^{-1}\right]$
η_{II}	Exergy efficiency $[\%]$
η_{I}	Energy efficiency $[\%]$